Scaling of the Molecular Weight-Dependent Thermal Volume Transition of Poly(*N*-isopropylacrylamide)

XIAODONG YE,[1] YANWEI DING,[2] JUNFANG LI[3]

[1]Department of Chemical Physics, University of Science and Technology of China, Hefei, Anhui 230026, China

[2]Hefei National Laboratory for Physical Sciences at Microscale, Structure Research Laboratory, University of Science and Technology of China, Hefei, Anhui 230026, China

[3]State Key Laboratory of Organometallic Chemistry, Shanghai Institute of Organic Chemistry, Chinese Academy of Sciences, 345 Ling Ling Road, Shanghai 200032, China

Received 3 February 2010; revised 19 March 2010; accepted 21 March 2010
DOI: 10.1002/polb.22018
Published online in Wiley InterScience (www.interscience.wiley.com).

ABSTRACT: A series of narrowly distributed poly(*N*-isopropylacrylamide) (PNIPAM) with molecular weight ranging from 8×10^4 to 2.3×10^7 g/mol were prepared by a combination of free radical polymerization and fractional precipitation. An ultrasensitive differential scanning calorimetry was used to study the effect of molecular weight on the thermal volume transition of these PNIPAM samples. The specific heat peak of the transition temperature ($T_{p,0}$) was obtained by extrapolation to zero heating rate (HR) because of the linear dependence of the transition temperature (T_p) on the HR. The relation between $T_{p,0}$ and the degree of polymerization (N) was investigated. © 2010 Wiley Periodicals, Inc. J Polym Sci Part B: Polym Phys 48: 1388–1393, 2010

KEYWORDS: degree of polymerization (DP); differential scanning calorimetry (DSC); dynamic light scattering; poly(*N*-isopropylacrylamide); stimuli-sensitive polymers

INTRODUCTION It is well known that poly(*N*-isopropylacrylamide) (PNIPAM) is soluble in water at low temperature and becomes insoluble at higher temperature above its lower critical solution temperature (LCST $\sim$ 32 °C).[1] PNIPAM has received much more attention because of its potential biomedical or pharmaceutical applications[2,3] as well as its application for the separation sciences[4] based on its thermosensitivity. The phase separation behavior for the aqueous solution of PNIPAM has been investigated by a variety of techniques including laser light scattering (LLS),[5–10] fluorescence,[11–13] differential scanning calorimetry (DSC),[14–21] turbidimetry,[18,19,21–23] and infrared spectroscopy.[24–26] Moreover, the phase transition of thermally sensitive homopolymers has also been investigated theoretically.[27–34] In spite of extensive experimental studies on the phase transition of PNIPAM, the issue about the molecular weight (M_w) dependence of phase transition is still controversial. Some studies show that the cloud point in turbidimetry studies or transition temperature in calorimetric measurements are dependent on M_w,[15,19,21,23] whereas others show that they are independent on M_w.[14,17,22] Recently, Xia et al.[19,21] synthesized several series of narrowly distributed PNIPAM with end groups of varying polarity by atom transfer radical polymerization (ATRP). Their results from turbidimetry and DSC clearly show that the M_w dependence could be seen as a combination of M_w and end group effects, that is, the aqueous solutions of narrow-disperse PNIPAMs with the same end group showed a dramatic decrease in cloud point with increasing M_w and the aqueous solutions of narrow-disperse PNIPAMs with more hydrophobic group but with the same M_w had lower cloud points.[19,21]

The results from theoretical studies are also controversial. On the basis of sequential hydrogen bond formation between polymer chains and water molecules, Tanaka and coworkers[27] reported phase diagrams with very flat LCST phase separation line, that is, cooperative hydration leads to flat LCST with almost no molecular weight dependence. On the other hand, it has been described by the mean field theory of Flory that there is a simple power law for the degree of polymerization (N) dependence of the critical temperature (T_c):[32]

$$T_c \propto N^{-1/2} \quad N \to \infty \tag{1}$$

Wilding et al.[33] concluded that the scaling of the critical temperature with chain length is well described by the same power law as the Flory theory (eq 1) by using configurational bias Monte Carlo methods. Yan et al.[34] also proved the validity of the Flory theory. More recently, Paul et al. studied the N dependence of maximum transition temperature using the Wang–Landau sampling idea.[29–31,35,36] They observed the predicted scaling behavior $T \sim N^{-1/2}$, where they used the peaks in the specific heat to determine the transition temperatures for different chain lengths.

Correspondence to: X. Ye (E-mail: xdye@ustc.edu.cn)

Until now, to our best knowledge, quantitative study on the M_w dependence of transition temperature by DSC experiments, especially in a broad range, has received less attention. In this article, a series of narrow-disperse PNIPAM was obtained by fractional precipitation following the conventional free radical polymerization using azobisisbutyronitrile (AIBN) as initiator. Our DSC results show that the transition temperature (T_p) had linear dependence on the heating rate (HR), so the $T_{p,0}$ was obtained by extrapolation to zero HR. The results show that $T_{p,0}$ have a scaling relation with the degree of polymerization (N) where the power is $-1/2$, which is consistent with the results described by Paul and coworkers.[29] Besides, from the data reported by Lessard et al.,[37] we found the same scaling law for poly(*N*,*N*-diethylacrylamide) homopolymers.

EXPERIMENTAL

Materials

Details for synthesis of the PNIPAM homopolymer can be found elsewhere.[7–9,38,39] Briefly, monomer *N*-isopropylacrylamide was recrystallized three times in a benzene/*n*-hexane mixture. The purified monomer and recrystallized AIBN as initiator were dissolved in purified solvent benzene. The solution was degassed through three cycles of freezing and thawing and the reaction was carried out at 56 °C for 30 h. The resultant PNIPAM homopolymer was carefully fractionated by a dissolution/precipitation process in a mixture of dry acetone and dry hexane at room temperature. The weight-average molar mass ($\langle M_w \rangle$) of PNIPAM fractions used were characterized by static light scattering. The distribution of four PNIPAM fractions with lower M_w was characterized by gel permeation chromatography (GPC) using a series of three linear Styragel columns HT3, HT4, and HT5. A Water 1515 pump and a Waters 2414 differential refractive index detector were used. The eluent was *N*,*N*-dimethylformamide with 1 g/L BrLi at a flow rate of 1.0 mL/min and narrowly distributed poly(ethylene oxide) (PEO) were used as standards. The polydispersity index (PDI, M_w/M_n) with higher M_w was estimated from the relative width $\mu_2/\langle\Gamma\rangle^2$ of the linewidth distribution measured in dynamic LLS by using $M_w/M_n \sim 1 + 4\mu_2/\langle\Gamma\rangle^2$.[40]

Laser Light Scattering

A spectrometer (ALV/DLS/SLS-5022F) equipped with a multi-τ digital time correlator (ALV5000) and a cylindrical 22 mW UNIPHASE He–Ne laser ($\lambda_0 = 632.8$ nm) as the light source was used. In static LLS,[40,41] we were able to obtain the weight-average molar mass (M_w) and the *z*-average root-mean-square radius of gyration [$(\langle R_g^2 \rangle^{1/2})$ or written as $\langle R_g \rangle$] in a very dilute solution from the angular dependence of the excess absolute scattering intensity.

$$\frac{KC}{R_{vv}(q)} \approx \frac{1}{M_w}\left(1 + \frac{1}{3}\langle R_g^2 \rangle_z q^2\right) + 2A_2C \qquad (2)$$

where $K = 4\pi^2 n^2 (dn/dC)^2/(N_A \lambda_0^4)$ and $q = (4\pi n/\lambda_0)\sin(\theta/2)$ with C, dn/dC, N_A, and λ_0 being the concentration of the polymer, the specific refractive index increment, the Avogadro's number, and the wavelength of light, respectively. The refractive index increment of PNIPAM was measured using a precise differential refractometer.[42] In dynamic LLS,[43] the Laplace inversion of a measured intensity–intensity time correlation function $G^{(2)}(t, q)$ in the self-beating mode can result in a line-width distribution $G(\Gamma)$. For a pure diffusive relaxation, Γ is related to the translational diffusion coefficient D by $\Gamma/q^2 = D$ at $q \to 0$ and $C \to 0$, or a hydrodynamic radius $R_h = k_B T/(6\pi\eta D)$ with k_B, T, and η being the Boltzman constant, absolute temperature, and solvent viscosity, respectively.

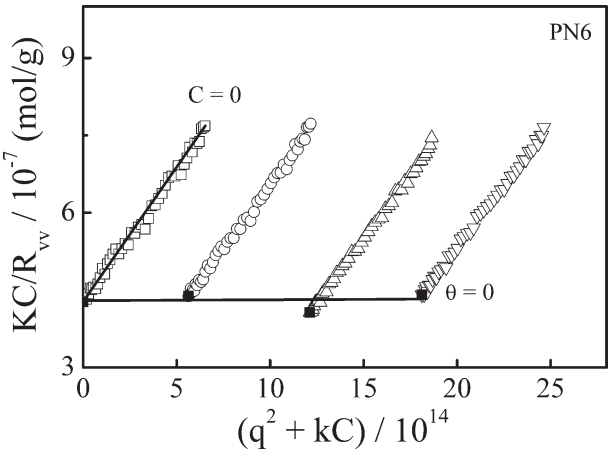

FIGURE 1 Typical Zimm plot of PN6 in aqueous solution at 25 °C, where C ranges from 9.40×10^{-2} to 3.02×10^{-1} g/L.

Differential Scanning Calorimetry

Ultrasensitive differential scanning calorimetry (US-DSC) measurements were carried on a VP-DSC from MicroCal. Both of the volumes of the sample and reference cells were 0.509 mL, respectively. The reference cell was filled with deionized water. PNIPAM solutions and the reference were degassed at 25 °C for half an hour. The solution was equilibrated at 10 °C for 2 h before the heating process. Data were analyzed using the software supplied by the manufacturer. The transition temperature (T_p) was taken as that corresponding to the maximum specific heat capacity ($C_{p,m}$) during the transition. The error of the transition temperature was within ±0.04 °C.

RESULTS AND DISCUSSION

A series of narrow-distribute PNIPAM with a broad range of molecular weight was prepared by a combination of conventional free radical polymerization and fractional precipitation. These PNIPAM samples were characterized by GPC or LLS. Figure 1 shows typical Zimm plots of PNIPAM sample (PN6). The extrapolation of $[KC/R_{vv}(q)]$ to $C \to 0$ and $q \to 0$ leads to M_w. Figure 2 shows typical normalized intensity–intensity correlation function and the corresponding distribution of hydrodynamic radius, which reveals that the PNIPAM fractions are narrowly distributed. Four PNIPAM samples with lower M_w were characterized by GPC and the other five PNIPAM samples were measured by LLS and the PDI was estimated from $M_w/M_n \sim 1 + 4\mu_2/\langle\Gamma\rangle^2$. The corresponding data are summarized in Table 1. From Table 1, we know that the distributions of all fractions are narrow. Note that for

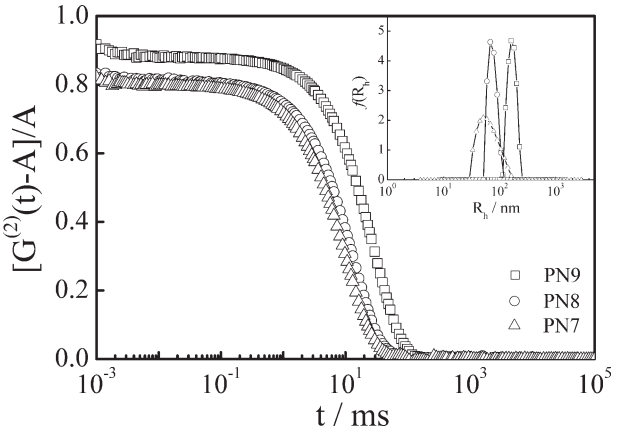

FIGURE 2 Typical measured intensity–intensity time correlation function $[G^{(2)}(t, q) - A]/A$ for PNIPAM fractions (PN7, PN8, and PN9). The inset shows corresponding hydrodynamic radius distribution $f(R_h)$.

PNIPAM fractions with lower molar mass, the M_w measured by LLS was smaller than that characterized by GPC. This phenomenon has also been observed by Schilli et al.[44] and Xia et al.[21] where they found that the M_w obtained by GPC were higher than those obtained from Matrix-assisted laser desorption/ionization-time of flight (MALDI-TOF) analysis and NMR method, respectively. In our experiments, narrowly distributed PEOs were used as standards, due to the possibly different chain conformations between the standards and PNIPAMs and/or the different interactions between column material/PEO and column materials/PNIPAM, the values measured by GPC can only be used to reveal the trend of the molecular weight and the distributions of the PNIPAMs. The molecular weight values determined by LLS from Zimm plots were used for further analyses in our work. Note that ^{1}H NMR and MALDI-TOF have also been used to characterize the molecular weights of PNIPAMs.[19,21,45–48] ^{1}H NMR spectroscopy has been used to obtain molecular weight by comparing the peak areas of the main chain with that arising from the end group. Xia et al.[21] has reported that the molecular weight values determined by ^{1}H NMR were in good agreement with theoretical values. However, if the signals from the end group overlap with those of the main chain or the molecular weights of PNIPAMs are so high that it is difficult to precisely integrate the area of the signals arising from the end group, the molecular weights cannot be determined by ^{1}H NMR under these circumstances. It has been reported that the values determined by MALDI-TOF are in good agreement with those from ^{1}H NMR[19] or theoretical calculation[49] for molecular weights below $\sim 4 \times 10^4$ g/mol. Ganachaud et al.[49] mentioned that it was difficult to analyze MALDI data at higher molecular weights because the PNIPAM tended to undergo fragmentation. Xia et al.[19] also reported that the PNIPAMs with molecular weight higher than 1×10^4 g/mol gave weak or nonexistent signals. Here, due to the broad range of molecular weight of PNIPAM, both MALDI-TOF and ^{1}H NMR are not good characterization methods.

Using these PNIPAM fractions with narrowly distributed M_w, we measured the phase transition by using US-DSC. In all measurements, the concentration of polymer was kept as 1 g/L. Our results showed that all data were reproducible.[20] Figure 3 shows the temperature dependence of specific heat capacity (C_p) at four different HRs of the PN8 fraction. From Figure 3, we know that T_p increased from 32.3 to 32.9 °C with increasing the HR from 0.081 to 1.49 °C/min, which may be due to the competition between intrachain contraction and interchain association in the HR[20] and/or may be due to the fact that a finite HR experiment is prone to sample nonequilibrium effects. Figure 4 shows T_p is in linear proportion to the HR, that is, $T_p = T_{p,0} + b \cdot \mathrm{HR}$. The $T_{p,0}$ values and the coefficients (b) for all PNIPAM samples have been summarized in Table 1. The b values did not change obviously with the molecular weight of PNIPAMs. Figure 5 shows that the temperature dependence of C_p for several PNIPAM fractions with different M_w. From Figure 5 and the $T_{p,0}$ values in Table 1, we know T_p has inverse M_w dependence, that is, the transition temperature decreases with increasing the M_w. Xia et al.[19,21] also found this same trend using five series of narrowly distributed PNIPAM prepared by ATRP. Similarly, Zhu and coworkers[37] have reported the inverse M_w dependence of LCST of poly(*N*,*N*-diethylacrylamide).

TABLE 1 Characterization of PNIPAM Samples by LLS, GPC, and US-DSC

	LLS		GPC		US-DSC	
Polymer	$\langle M_w \rangle$ (10^4 g/mol)	M_w/M_n	$\langle M_w \rangle$ (10^4 g/mol)	M_w/M_n	$T_{p,0}$/°C	b/min
PN1	8		17	1.16	33.99	0.44
PN2	15		24	1.19	33.67	0.49
PN3	42		61	1.19	32.93	0.38
PN4	64		91	1.16	32.67	0.35
PN5	120	1.5			32.48	0.30
PN6	240	1.4			32.45	0.36
PN7	390	1.5			32.35	0.41
PN8	770	1.4			32.32	0.43
PN9	2300	1.2			32.26	0.40

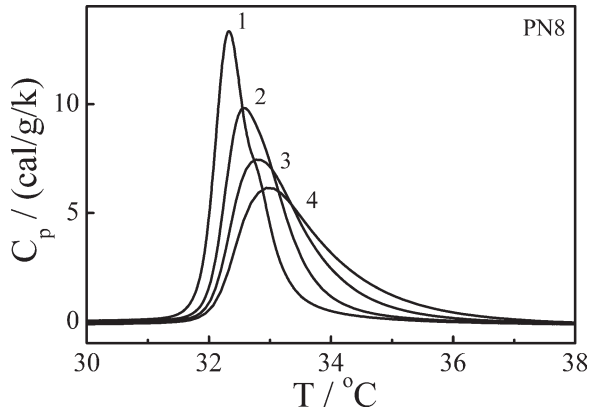

FIGURE 3 Effect of heating rate on the thermal volume transition of PN8 in water where the heating rate was (1) 0.081, (2) 0.50, (3) 1.00, and (4) 1.49 °C/min.

Theoretically, by the mean field theory of Flory,[32] we know the critical temperature (T_c) is scaled to the degree of polymerization (N), that is, $T_c \propto N^{-1/2}$. Wilding et al.[33] and Yan et al.[34] proved the validity of the Flory theory by using configurational bias Monte Carlo Methods and an expanded grand canonical ensemble simulation, respectively. It should be noted that critical temperature T_c is different from the T_p measured by DSC. At T_c, the solution separates into two phases with different compositions. T_p is the temperature where the specific heat capacity reaches its maximum. Using the Wang–Landau sampling idea,[35,36] Paul et al. have shown that the specific heat peak for the coil-to-globule transition, that is, T_p here, is proportional to $N^{-1/2}$.[29–31] Thus, the $T_{p,0}$ values in Table 1 have been plotted in Figure 6(a). For the first time, we experimentally found the $T_{p,0}$ measured by DSC experiments is proportional to $N^{-1/2}$. From Figure 6(a), the intercept T_0 and the slope were 32.08 ± 0.05 and 52 ± 3 °C, respectively. To confirm the scaling relation between $T_{p,0}$ and N, the data in Figure 6(a) have been replotted in Figure 6(b) in the form of $\ln(T_{p,0} - T_0)$ versus $\ln N$. From

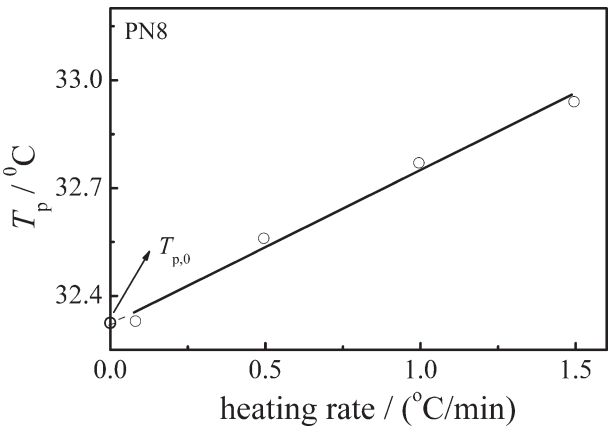

FIGURE 4 Heating rate dependence of transition temperature (T_p) of PNIPAM fraction PN8.

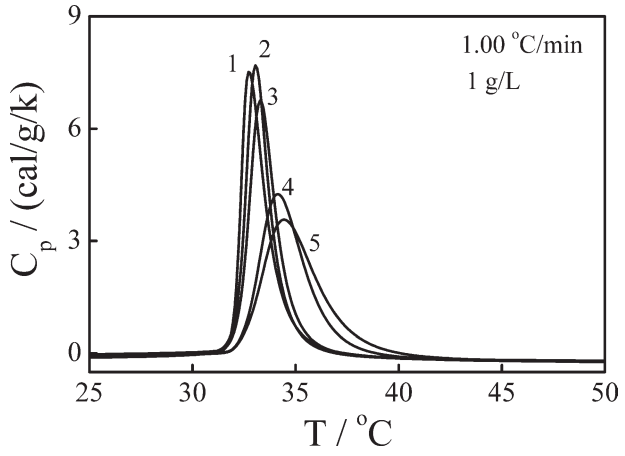

FIGURE 5 Effect of molecular weight on the thermal volume transition of PNIPAM chains in water where the heating rate was 1.00 °C/min. Curves 1–5: (1) PN7, (2) PN4, (3) PN3, (4) PN2, and (5) PN1.

Figure 6(b), we know that the slope, that is, the power, was −0.44 ± 0.04 that is close to −1/2. By turbidimetry and DSC, Xia et al.[19,21] have measured the thermal response of

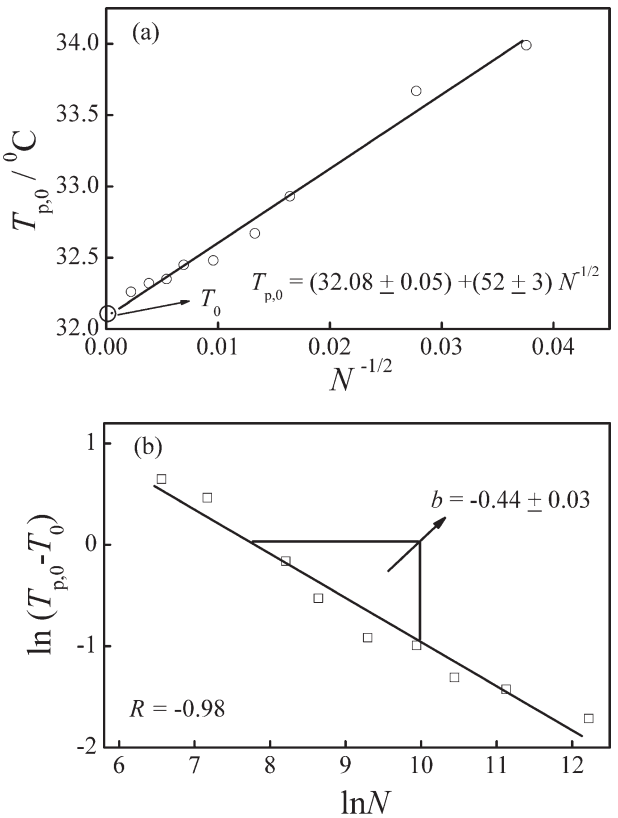

FIGURE 6 (a) A plot of $T_{p,0}$ versus $N^{-1/2}$, where N is the degree of polymerization of PNIPAM and the concentration of all PNIPAM fractions in water was 1 g/L. (b) A plot of natural logarithm of the ($T_{p,0} - T_0$) as a function of the natural logarithm of N.

several series of narrow-disperse PNIPAM synthesized by ATRP. Winnik and coworkers[48] synthesized three linear PNIPAMs with an azido group on one end and propargyl group on the other end by reversible addition-fragmentation chain transfer and characterized the phase transition of these samples by DSC. We found the instruments used by us, Xia et al., and Winnik et al. are VP-DSC microcalorimeters from MicroCal, so we put their data in Figure 7 together with our data just to reveal the trend due to the fact that the molecular weights from different groups were determined by different characterization methods. The dashed lines are guides for the eyes. In the experiments reported by Xia et al.[21] 2-chloropropionamide (CP), *N*-isopropyl-2-chloropropionamide (*i*-PrCP), ethyl 2-chloropropionate (ECP), and *N*-phenyl-2-chloropropionamide (PhCP) were used as initiators to give polymers with end groups of varying polarity, ranging from hydrophilic for CP to hydrophobic for PhCP. From Figure 7, we know that when $N^{-1/2}$ is smaller than ~0.11, that is, M_w is larger than ~9300 g/mol and N is larger than ~83, all the data are closed to the dash line expect the PNIPAMs with more hydrophobic end groups ECP and PhCP. We also observed that although the T_p of PNIPAMs with end group PhCP is lower than those of PNIPAMs with other more hydrophilic end groups, T_p is also proportional to $N^{-1/2}$. When the N is smaller than ~83, the data deviated from the dash line may be due to the higher order corrections [i.e., O(N)].[29] Similarly, using Wang–Landau sampling idea, Paul and coworkers[29] also observed deviations of the positions of the specific heat peaks from the $N^{-1/2}$ behavior in the finite N.

Lessard et al.[37] have studied the effect of molecular weight on the LCST of poly(*N*,*N*-diethylacrylamide). Their data have been replotted in Figure 8(a). From Figure 8(a), we know that for poly(*N*,*N*-diethylacrylamide), a same and simple scaling law exists between T_p and N, that is, $T_p \propto N^{-1/2}$. The intercept T_0 and the slope were 27.6 °C and 102 °C, respectively. Note that the molecular weight and the distribution of the polymer samples were precisely determined by size exclusion chromatography on a Waters system equipped with an online differential refractometer by using polystyrene samples as the standards. Figure 8(b) shows that a plot of natural logarithm of the $(T_p - T_0)$ as a function of the natural logarithm of the degree of polymerization (N). The slope is −0.57, which is also close to −1/2, indicating that existence of the scaling relation between T_p and N for this thermally sensitive homopolymer.

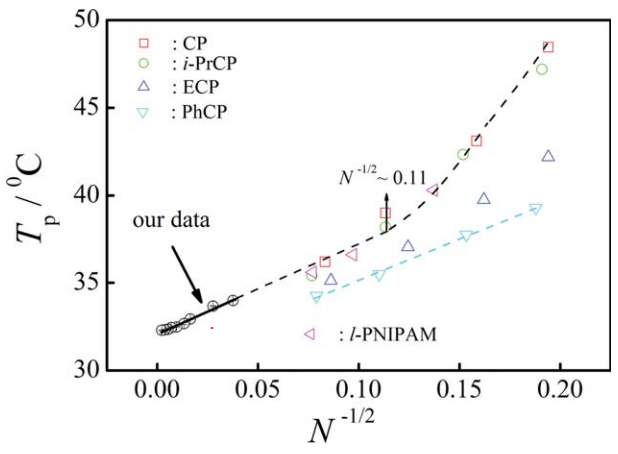

FIGURE 7 Plots of $T_{p,0}$ from our experiments and T_p from refs. 21 and 48, the lines are guides for eyes.

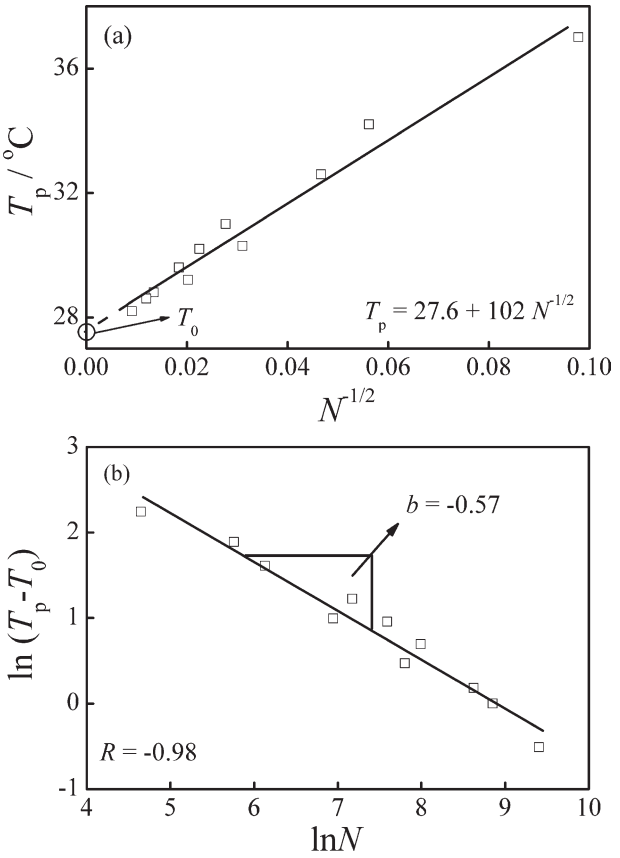

FIGURE 8 Replots of the data presented in Table 1 of ref. 37: (a) A plot of T_p of poly(*N*,*N*-diethylacrylamide) versus $N^{-1/2}$. (b) A plot of natural logarithm of the $(T_p - T_0)$ as a function of the natural logarithm of N.

CONCLUSIONS

By using a combination of free radical polymerization and fractional precipitation, a series of PNIPAM with narrowly distributed molar mass has been prepared. DSC measurements show that the $T_{p,0}$ is proportional to $N^{-1/2}$, which is consistent with theoretical results from Paul et al. Besides, poly(*N*,*N*-diethylacrylamide) has the same scaling relation between T_p and N.

The authors thank Prof. Guangzhao Zhang for his valuable comments about the manuscript and interpretation of our results. The financial support of the National Natural Scientific Foundation of China (NNSFC) Projects (20804043), Specialized Research Fund for the Doctoral Program of Higher Education (200803581022), and the Fundamental Research Funds for the Central Universities is gratefully acknowledged.

REFERENCES AND NOTES

1 Schild, H. G. Prog Polym Sci 1992, 17, 164–249.

2 Jeong, B.; Kim, S. W.; Bae, Y. H. Adv Drug Delivery Rev 2002, 54, 37–51.

3 Schmaljohann, D. Adv Drug Delivery Rev 2006, 58, 1655–1670.

4 Kikuchi, A.; Okano, T. Prog Polym Sci 2002, 27, 1165–1193.

5 Kubota, K.; Fujishige, S.; Ando, I. J Phys Chem 1990, 94, 5154–5158.

6 Meewes, M.; Ricka, J.; de Silva, M.; Nyffenegger, R.; Binkert, T. Macromolecules 1991, 24, 5811–5816.

7 Wu, C.; Zhou, S. Q. Macromolecules 1995, 28, 8381–8387.

8 Wu, C.; Zhou, S. Q. Phys Rev Lett 1996, 77, 3053–3055.

9 Wu, C.; Zhou, S. Q. Macromolecules 1995, 28, 5388–5390.

10 Wang, X. H.; Qiu, X. P.; Wu, C. Macromolecules 1998, 31, 2972–2976.

11 Winnik, F. M. Macromolecules 1990, 23, 233–242.

12 Ringsdorf, H.; Venzmer, J.; Winnik, F. M. Macromolecules 1991, 24, 1678–1686.

13 Schild, H. G.; Tirrell, D. A. Langmuir 1991, 7, 665–671.

14 Otake, K.; Inomata, H.; Mikio, K.; Saito, S. Macromolecules 1990, 23, 283–289.

15 Schild, H.; Tirrell, D. A. J Phys Chem 1990, 94, 4352–4356.

16 Tiktopulo, E. I.; Bychkova, V. E.; Rička, J.; Ptitsyn, O. B. Macromolecules 1994, 27, 2879–2882.

17 Tiktopulo, E. I.; Uversky, V. N.; Lushchik, V. B.; Klenin, S. I.; Bychkova, V. E.; Ptitsyn, O. B. Macromolecules 1995, 28, 7519–7524.

18 Boutris, C.; Chatzi, E. G.; Kiparissides, C. Polymer 1997, 38, 2567–2570.

19 Xia, Y.; Yin, X. C.; Burke, N. A. D.; Stöver, H. D. H. Macromolecules 2005, 38, 5937–5943.

20 Ding, Y. W.; Ye, X. D.; Zhang, G. Z. Macromolecules 2005, 38, 904–908.

21 Xia, Y.; Burke, N. A. D.; Stöver, H. D. H. Macromolecules 2006, 39, 2275–2283.

22 Fujishige, S.; Kubota, K.; Ando, I. J Phys Chem 1989, 93, 3311–3313.

23 Tong, Z.; Zeng, F.; Zheng, X.; Sato, T. Macromolecules 1999, 32, 4488–4490.

24 Maeda, Y.; Higuchi, T.; Ikeda, I. Langmuir 2000, 16, 7503–7509.

25 Maeda, Y.; Nakamura, T.; Ikeda, I. Macromolecules 2001, 34, 1391–1399.

26 Katsumoto, Y.; Tanaka, T.; Sato, H.; Ozaki, Y. J Phys Chem A 2002, 106, 3429–3435.

27 Okada, Y.; Tanaka, F. Macromolecules 2005, 38, 4465–4471.

28 Mendez, S.; Curro, J. G.; McCoy, J. D.; Lopez, G. P. Macromolecules 2005, 38, 174–181.

29 Ramf, F.; Binder, K.; Paul, W. J Polym Sci Part B: Polym Phys 2006, 44, 2542–2555.

30 Paul, W.; Strauch, T.; Rampf, F.; Binder, K. Phys Rev E 2007, 75, 060801(R).

31 Taylor, M. P.; Paul, W.; Binder, K. J Chem Phys 2009, 131, 114907-1–114907-9.

32 Flory, P. J. Principles of Polymer Chemistry; Cornell University Press: Ithaca, 1953.

33 Wilding, N. B.; Müller, M.; Binder, K. J Chem Phys 1996, 105, 802–809.

34 Yan, Q. L.; de Pablo, J. J. J Chem Phys 2000, 113, 5954–5957.

35 Wang, F.; Landau, D. P. Phys Rev Lett 2001, 86, 2050–2053.

36 Wang, F.; Landau, D. P. Phys Rev E 2001, 64, 056101.

37 Lessard, D. G.; Ousalem, M.; Zhu, X. X. Can J Chem 2001, 79, 1870–1874.

38 Zhou, S. Q.; Fan, S. Y.; Au-yeung, S. T. F.; Wu, C. Polymer 1995, 36, 1341–1346.

39 Ye, X. D.; Lu, Y. J.; Shen, L.; Ding, Y. W.; Liu, S. L.; Zhang, G. Z.; Wu, C. Macromolecules 2007, 40, 4750–4752.

40 Chu, B. Laser Light Scattering, 2nd ed.; Academic Press: New York, 1991.

41 Zimm, B. H. J Chem Phys 1948, 16, 1099–1115.

42 Wu, C.; Xia, K. Q. Rev Sci Instrum 1994, 65, 587–590.

43 Berne, B. J.; Pecora, R. Dynamic Light Scattering; Wiley-Interscience: New York, 1976.

44 Schilli, C.; Lanzendörfer, M. G.; Müller, A. H. E. Macromolecules 2002, 35, 6819–6827.

45 Heredia, K. L.; Grover, G. N.; Tao, L.; Maynard, H. D. Macromolecules 2009, 42, 2360–2367.

46 Grover, G. N.; Alconcel, S. N. S.; Matsumoto, N. M.; Maynard, H. D. Macromolecules 2009, 42, 7657–7663.

47 Qiu, X. P.; Winnik, F. M. Macromolecules 2007, 40, 872–878.

48 Qiu, X. P.; Tanaka, F.; Winnik, F. M. Macromolecules 2007, 40, 7069–7071.

49 Ganachaud, F.; Monteiro, M. J.; Gilbert, R. G.; Dourges, M. A.; Thang, S. H.; Rizzardo, E. Macromolecules 2000, 33, 6738–6745.